Solar-powered adsorption-based multi-generation system working under the climate conditions of GCC countries: theoretical investigation.

EL-SHARKAWY, I.I., HASSAN, M., ABD-ELHADY, M.M., RADWAN, A. and INAYAT, A.

2023

Article

Solar-Powered Adsorption-Based Multi-Generation System Working under the Climate Conditions of GCC Countries: Theoretical Investigation

Ibrahim I. El-Sharkawy [1,2,*], **M. Hassan** [3,4], **Mahmoud M. Abd-Elhady** [5], **Ali Radwan** [1] **and Abrar Inayat** [1]

1. Sustainable and Renewable Energy Engineering Department, College of Engineering, University of Sharjah, Sharjah 27272, United Arab Emirates
2. Mechanical Power Engineering Department, Faculty of Engineering, Mansoura University, El-Mansoura 35516, Egypt
3. Department of Mechanical Engineering, College of Engineering, Jazan University, Jazan 82812, Saudi Arabia
4. Department of Mechanical Engineering, Faculty of Energy Engineering, Aswan University, Aswan 81528, Egypt
5. Department of Mechanical Engineering, Faculty of Engineering, Damietta University, New Damietta 34517, Egypt.eg
* Correspondence: ielsharkawy@sharjah.ac.ae

Abstract: In this study, transient modelling for a solar-powered adsorption-based multi-generation system working under the climatic conditions of the Gulf Cooperation Council (GCC) countries is conducted. Three cities are selected for this study: Sharjah in the United Arab Emirates, Riyadh in Saudi Arabia, and Kuwait City in Kuwait. The system comprises (i) evacuated tube solar collectors (ETCs), (ii) photovoltaic-thermal (PVT) solar collectors, and (iii) a single-stage double-bed silica gel/water-based adsorption chiller for cooling purposes. A MATLAB code is developed and implemented to theoretically investigate the performance of the proposed system. The main findings of this study indicate that among the selected cities, based on the proposed systems and the operating conditions, Riyadh has the highest cooling capacity of 10.4 kW, followed by Kuwait City, then Sharjah. As for the coefficient of performance (COP), Kuwait City demonstrates the highest value of 0.47. The electricity generated by the proposed system in Riyadh, Kuwait City, and Sharjah is 31.65, 31.3, and 30.24 kWh/day, respectively. Furthermore, the theoretical results show that at 18:00, the overall efficiency of the proposed system reaches about 0.64 because of the inclusion of a storage tank and its feeding for the adsorption chiller. This study analyzes the feasibility of using a combination of ETCs and PVT collectors to drive the adsorption chiller system and produce electricity in challenging weather conditions.

Keywords: adsorption cooling; electricity generation; GCC countries; multi-generation system; evacuated tube solar collectors; solar energy

1. Introduction

Cooling has become an essential necessity, particularly in regions known for hot climates, such as tropical and equatorial countries. Elevated temperatures and humidity levels can significantly influence daily life in these regions. Global warming is also affecting regions worldwide, with a resultant increase in the mean temperatures all over the planet [1]. Also, population growth and rising living standards are driving an additional need for cooling and air conditioning systems, which are becoming increasingly common [2], particularly compression cooling systems, due to their notable efficiency and comparatively affordable cost. However, these systems consume a significant portion of worldwide electricity, primarily generated by burning fossil fuels [3]. Therefore, compression-based cooling systems have harmful environmental effects, contributing to increasing global carbon emissions. The International Institute of Refrigeration (IIR) estimated that the electrical

energy consumed by refrigeration systems represents approximately 20% of the global electrical power consumption [4]. Specifically, air-conditioning units consume about 8.5% of the world's total electricity, emitting one gigaton of carbon dioxide into the atmosphere [5].

Therefore, there is a need for sustainable and renewable cooling systems, particularly those powered by renewable and clean energy resources. The Gulf Cooperation Council (GCC) countries have abundant access to solar energy. For instance, the United Arab Emirates (UAE) has an average annual solar radiation of 2285 kWh/m^2, with a daily sunshine duration of 10 h, while Kuwait has an average yearly solar radiation of 2150 kW/m^2, with an average daily sunshine duration ranging from 7 to 12 h, and the yearly average solar radiation for Saudi Arabia has a value of 2200 kWh/m^2 [6]. This availability makes solar energy a viable and environmentally friendly renewable source in these regions. Hence, the ideal solution for the cooling demand problem in these regions is the implementation of systems that can not only fulfill the necessary cooling capacity, but also generate electrical energy. Solar-powered multigenerational systems, rather than conventional ones, have emerged as one of the most effective methodologies to address this issue.

As a part of the proposed system, adsorption cooling systems powered by renewable sources offer the benefit of using natural refrigerants for cooling purposes, which have no negative effects on global warming and may be driven by low-temperature solar energy sources [1,7]. Additionally, they have a lifespan of around 25 years, can operate at temperatures above 50 °C, require less maintenance as they do not have moving parts, and do not experience crystallization or corrosion issues [8]. However, these systems have comparatively low coefficients of performance (COP). Adsorption chillers driven by renewable energy have recently received much interest for their use in heating and cooling generation [9]. Moreover, using clean and renewable energy sources, such as solar, to power these systems reflects the long-term answer to this issue [10–12]. Due to their capacity to simultaneously produce electricity and deliver solar thermal energy, photovoltaic-thermal (PVT) collectors have been gaining popularity in different research areas [13,14]. In the PVT collectors, high electrical efficiency can be attained compared to the conventional PV modules due to the temperature reduction of the PV modules in the PVT collectors. Therefore, PVT collectors show higher overall solar energy conversion.

Many researchers have studied different configurations of multi-generation and hybrid solar-powered adsorption-based systems [1,15]. For instance, Mohammadi et al. [16] reviewed the different configurations of solar-powered multigeneration systems, including adsorption chillers. Hassan et al. [17] theoretically evaluated the performance of five distinct multi-generation system configurations. Additionally, a techno-economic evaluation of a solar-powered adsorption cooling system was carried out [18]. A multigeneration system was investigated by Calise et al. [19] utilizing a PVT collector, an adsorption cooling system, and a solar-assisted heat pump. The PVT collector's efficiency was 49%, the adsorption chiller's COP was 0.55, and the heat pump's COP was 4, according to the findings. In El-Sharkawy et al. [20], the potential use of solar-driven adsorption chillers using the Middle East's climate conditions was theoretically studied. A two-bed system using silica gel and water was driven by a compound parabolic solar collector. The performance of this proposed setup was explored theoretically. Furthermore, in Papoutsis et al. [21], a theoretical analysis was performed on three unique solar-driven cooling systems. The first system employs a standard electric chiller powered by different PV panels. The second system utilizes a solar-driven adsorption cooling mechanism. Meanwhile, the third system is a hybrid model that combines adsorption and electric chillers, powered by PVT collectors. Mostafa et al. [22] formulated a mathematical representation for a solar-powered adsorption cooling system tailored for cold storage applications. A monthly evaluation of the system's performance metrics was conducted together with an economic analysis. The research showed the system's proficiency in hot and dry weather conditions. It was observed that both the performance factor and the initial energy ratio excelled in such climates. In hot and arid conditions, the cooling cost averaged USD 0.203/kWh, while in humid regions, it stood at USD 0.485/kWh.

Based on the previously mentioned viewpoints, many past studies have concentrated on utilizing either solar thermal collectors or thermal photovoltaic collectors to power adsorption chillers. However, the system that we introduce here presents a new setup that leverages the optimal combination of PVT and evacuated tube collectors (ETCs), both to drive an adsorption chiller and generate electricity. This amalgamation was determined by investigating five configurations of PVT/ETC arrangements conducted in one of our previous studies [17]. This system's performance when operated under the weather conditions of the GCC countries was theoretically investigated. Three cities in the GCC countries were selected for this study: Sharjah in the UAE, Riyadh in Saudi Arabia, and Kuwait City in Kuwait. This research was undertaken during the summer months, specifically June, July, and August, of these cities. The cooling was generated through a single-stage, dual-bed adsorption cooling system powered by solar thermal energy and employing a silica gel/water pair. The dynamic performance of the proposed system was analyzed using a prepared MATLAB code. To generate electricity throughout the year and harness solar thermal energy, commercially certified ETCs and PVT collectors were used.

2. Description of the Proposed System

Figure 1 displays the layout of the system proposed in this study. The system comprises (i) ETCs, (ii) PVT collectors, and (iii) a single-stage, dual-bed adsorption cooling unit that employs a silica gel/water pair. The PVT module generates electricity for both the building and system pumps, while the ETCs are used to drive the adsorption cooling system. The technical specifications for the ETCs and PVT collectors were obtained from the Apricus company in the USA and FOTOTHERM in Italy, respectively [23,24]. Table 1 summarizes the technical details of these collectors.
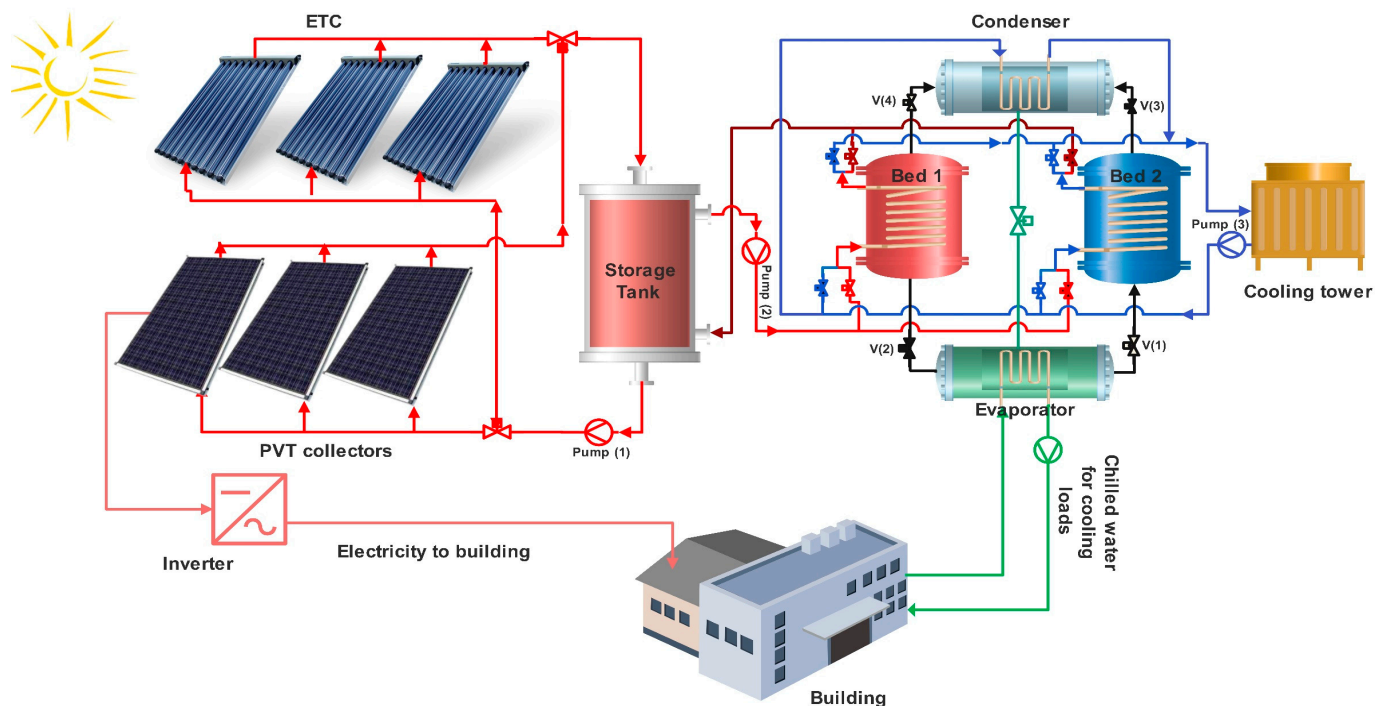
Figure 1. Schematic diagram of the proposed system.

The adsorption cooling unit is driven by thermal energy generated by the PVT/ETC solar collector arrangement. A hot water storage tank is implemented between the solar collector arrangement and adsorption chillers to reduce the negative impacts of solar energy fluctuations (see Figure 1). It should be highlighted that water flows through the PVT collectors, and the ETCs are in a parallel scheme. The water exits from both the PVT and the solar collectors and is then directed to the storage tank.

Table 1. Technical specifications of the utilized PVT collectors and ETCs [23,24].

FOTOTHERM PVT.		Apricus (ETC-20) ETC.	
■ Thermal Specifications		■ Thermal Specifications	
Aperture Area	1.58 m^2	Aperture Area	1.89 m^2
Optical Efficiency (η_0)	58.3%	Optical Efficiency (η_0)	71.4%
Heat loss coefficient (c_1)	6.08 W m^{-2} K^{-2}	Heat loss coefficient (c_1)	1.243 W m^{-2} K^{-1}
Heat loss coefficient (c_2)	0.0 W m^{-2} K^{-2}	Heat loss coefficient (c_2)	0.009 W m^{-2} K^{-2}
■ Electrical Specifications			
Type of Cell	Monocrystalline		
Nominal power	300 W$_p$		
efficiency of Module	18.3%		
Power Temperature coefficient	-0.40% °C^{-1}		

The adsorption cooling unit's operation comprises four main modes, which can be summarized as follows:

Mode (A): In this mode, bed (1) is connected to the evaporator through valve V(1), and disconnected from the condenser by closing valve V(3). The water vapor, the refrigerant, flows from the evaporator to the adsorber heat exchanger (bed (1)) and is adsorbed by the silica gel (silica gel). The heat of adsorption is rejected by the cooling water that flows through bed (1). In this process, the cooling load is generated inside the evaporator due to the evaporation of water vapor. Simultaneously, bed (2) is connected to the condenser through valve V(4) and disconnected from the evaporator by closing valve V(2). Hot water flows through bed (2), where the refrigerant is regenerated and flows to the condenser where condensation occurs. The condensed refrigerant runs to the evaporator through a throttling valve.

Mode (B): In this mode, both beds are disconnected from the evaporator and the condenser. Hot water flows to bed (1), where its pressure increases from the pressure of the evaporator to that of the condenser, in a process named the pre-heating process. Simultaneously, cooling water flows through bed (2), where its pressure drops from the condenser pressure to the evaporator pressure, in a process named the pre-cooling process.

Mode (C): This mode can be considered as the reverse of mode (A), wherein bed (1) is linked to the condenser while being separated from the evaporator. Bed (2) is connected to the evaporator and disconnected from the condenser.

Mode (D): This mode is the opposite of mode (B).

3. Mathematical Model

3.1. Solar Collectors

3.1.1. Thermal Performance

Equation (1) provides the energy balance for the ETCs and PVT collectors. The PVT collector can be considered a common solar thermal collector, whose PV layer covers the absorber. Certain presumptions are used to streamline the model and provide a suitable thermal description of the PVT collectors. These assumptions are (i) one-dimensional heat transfer and (ii) thermal equilibrium between the absorber surface and the PV layer [25,26]. The heat balance for solar collectors can be analyzed using Equation (1) given below [20]:

$$\left(mC_p\right)_{s.c} \frac{dT_{s.c}}{dt} = I_t . A_{s.c} . \eta_{th,\,s.c} + \dot{m}_w C_{p_{r_w}} \left(T_{w,s.c,in} - T_{w,s.c,out}\right) \tag{1}$$

As for ETCs and PVT collectors, the thermal efficiency, $\eta_{th,solar}$, can be estimated using Equation (2) as a function of the solar radiation, ambient temperature, and the

average temperature of heat transfer fluid ($\overline{T}_{mean,w}$), which can be calculated by $T_{mean,w} = (T_{w,s,in} + T_{w,s,out})/2$ [20].

$$\eta_{th,solar} = \eta_{0pt} - C_1 \left(\frac{T_{mean,s.c,w} - T_{amb}}{I_t} \right) - C_2 \left(\frac{(T_{mean,\ s.c,w} - T_{amb})^2}{I_t} \right) \tag{2}$$

where, C_1 and C_2 are the heat loss coefficients, which are previously calculated for the solar collector's manufacturer model, and η_{0pt} is the optical efficiency defined in Equation (3) [27],

$$\eta_{0pt} = \rho.\,\tau.\alpha.\gamma.k \tag{3}$$

where ρ is the mirror reflectivity, τ is the cover transmittance, α is the absorber solar absorptivity, γ is the intercept factor, and k is the incidence angle modifier.

3.1.2. Electrical Performance (PVT Performance)

By evaluating the PVT solar collector's electrical efficiency, the electrical power generated by the PVT collectors is depicted. Manufacturers of PVT collectors supply a reference value for this electrical efficiency ($\eta_{Ref,el}$) that is computed based on a standard testing condition, where the (I_t) is 1000 W/m^2 and the reference temperature (T_{ref}) is 25 °C [28]. This value, given by Equation (4), is then applied to calculate the actual electrical efficiency ($\eta_{Act,el}$) [17].

$$\eta_{Ref,\ el} = \frac{P_{el}}{A_{PVT}.I_t} \tag{4}$$

where A_{PVT} is the PVT collectors' aperture area and P_{el} is the electrical power generated instantly by the PVT collectors. However, during the day, there are regular fluctuations in the solar radiation incidence circumstances as well as the temperature of the solar cells. Equation (5) is used to estimate the value of $\eta_{Act,el}$ at various I_t and T_{cell} [28].

$$\eta_{Act,\ el} = \eta_{Ref,el} \left[1 - \beta \left(T_{cell} - T_{ref} \right) \right] \tag{5}$$

where β is the power's temperature coefficient, which is supplied by the manufacturer.

3.2. The Storage Tank

The energy balance on the hot water storage tank is calculated by Equation (6) as in El-Sharkawy et al. [20],

$$(mC_p)_{s,t} \frac{dT_{s.t}}{dt} = \dot{Q}_{s.c} - \left[\dot{Q}_{reg.ad} + \dot{Q}_{surr} \right] \tag{6}$$

where $\dot{Q}_{s.c}$ is the thermal energy delivered by the collector, $\dot{Q}_{reg,ad}$ stands for the thermal energy needed to drive the regeneration process of the adsorption chiller, and $\dot{Q}_{surr}$ is the thermal energy lost to the environment. Their values can be calculated using Equations (7)–(9) [20]:

$$\dot{Q}_{s.c} = \dot{m}_{hw,s.c}.\,c_{P,hw.s.c}. \left[T_{hw,s.c,out} - T_{hw,s.c,in} \right] \tag{7}$$

$$\dot{Q}_{reg.\ ad} = \dot{m}_{hw,ad}.\,c_{P,hw}. \left[T_{hw,in} - T_{hw,out} \right] \tag{8}$$

$$\dot{Q}_{surr} = U_{surr}.\,A_{s.t}. \left[T_{s.t} - T_{amb} \right] \tag{9}$$

3.3. Adsorption Chiller

The adsorption chiller is mathematically modeled by simultaneously resolving the equilibrium and kinetics of silica gel/water adsorption and the energy balance of ad-

sorption/desorption heat exchangers, the condenser, and the evaporator. The following presumptions are used in this context [29]:

- The main system piping lines and components are well insulated.
- At saturation conditions, the evaporator's and condenser's outlet statuses are taken into consideration.
- The system pumping power is disregarded, and the water flow inside the pipe is a continuous, steady 1D flow.

3.3.1. Silica Gel/Water Adsorption Equilibrium and Kinetics

The widely accepted linear driving force (LDF) equation is employed to estimate the adsorption kinetics in the context of the silica gel–water pair [30–32].

$$\frac{dw}{dt} = K(W_{eq} - w) \tag{10}$$

where K is the mass transfer coefficient, which is obtained from the following equation.

$$K = \frac{15 D_{so} \exp\left(-\frac{E_a}{RT}\right)}{r_p^2} \tag{11}$$

In the above equation, R represents the universal gas constant, r_p represents the radius of the silica gel particles, E_a is the activation energy, and D_{so} stands for the pre-exponential constant. The numerical values of E_a and D_{so} for the silica gel–water pair are widely used and are 4.48×10^4 J/mol and 2.54×10^{-4} m^2/sec, respectively [32]. The silica gel particle radius is 1.72×10^{-4} m.

To assess the adsorption equilibrium of the silica gel–water pair, as in Equation (12), the modified Freundlich equation [30] is utilized.

$$W_{eq} = A(T_s) \left[\frac{P_{sat}(T_w)}{P_{sat}(T_s)} \right]^{B(T_s)} \tag{12}$$

where

$$A(T_s) = \sum_{n=o}^{3} A_n T_s^n \tag{13}$$

$$B(T_s) = \sum_{n=o}^{3} B_n T_s^n \tag{14}$$

where T_s represents the temperature of the adsorbent, while A_n and B_n are constant coefficients. These coefficients are given in Table 2.

Table 2. Constants of the silica gel/water adsorption equilibrium [30] (reprinted with permission from Elsevier).

Parameter	Value	Unit
A_0	-6.5314	kg.kg^{-1}
A_1	0.072452	kg.kg^{-1}.K^{-1}
A_2	-0.23951×10^{-3}	kg.kg^{-1}.K^{-2}
A_3	0.25493×10^{-6}	kg.kg^{-1}.K^{-3}
B_0	-15.587	---
B_1	0.15915	K^{-1}
B_2	-0.50612×10^{-3}	K^{-2}
B_3	0.5329×10^{-6}	K^{-3}

3.3.2. Energy Balance of Adsorption Beds

Using lumped parameter modelling, the energy balance of adsorption beds is simulated. Equation (15) represents the energy balance for the bed in its adsorption process, whereas Equation (16) represents the energy balance for the bed in desorption mode [20].

$$\left(\sum_i m_i c_{P,i}\right)\frac{dT}{dt} = \emptyset.m_{ad}\left(\frac{dw}{dt}\right)(Q_{st}) - \left(\dot{m}c_p\right)_{cw}(T_{cw,out} - T_{cw,in}) \tag{15}$$

$$\left(\sum_i m_i c_{P,i}\right)\frac{dT}{dt} = \emptyset.m_{ad}\left(\frac{dw}{dt}\right)(Q_{st}) - \left(\dot{m}c_p\right)_{hw}(T_{hw,out} - T_{hw,in}) \tag{16}$$

where the flag $\emptyset$ is a variable that is set to 0 during switching processes and subsequently set to 1 during adsorption or desorption processes. The summation term in Equations (15) and (16) represents all of the bed elements, containing the adsorbent, adsorbate, and heat exchanger material.

3.3.3. Energy Balance of the Evaporator and Condenser

Equations (17) and (18), respectively, represent the energy balance equations for the evaporator and condenser.

$$\left(mc_p\right)_{eva}\frac{dT}{dt} = -\emptyset.h_{fg}M_{ad}\frac{dw_{ad}}{dt} - \left(\dot{m}c_p\right)_{ch}(T_{ch,out} - T_{ch,in}) \tag{17}$$

$$\left(mc_p\right)_{con}\frac{dT}{dt} = \emptyset.h_{fg}.m_{ad}\frac{dw_{de}}{dt} - \left(\dot{m}c_p\right)_{con}(T_{c,out} - T_{c,in}) \tag{18}$$

The flag's numerical values $\emptyset$ are comparable to those in Equations (15) and (16). The logarithmic mean temperature difference (LMTD) method is used to estimate the outlet temperatures of four components including the two beds, the condenser, and the evaporator. Equation (19) represents a general formula for the LMTD method [17]:

$$T_{HE,Out} = T_{HE} + (T_{HE,in} - T_{HE,})exp\left[\frac{-UA_{HE}}{\dot{m}_w c_{p,w}}\right] \tag{19}$$

where *HE* represents the four systems' heat exchangers. Table 3 includes the four component's mass flow rate, total thermal conductance, and thermal conductance.

Table 3. Numerical values of adsorption chiller parameters used in the simulation [20].

Parameter	Value	Units
M_{ads}	47	kg
$M_{cu,bed}$	51.2	Kg
$M_{Al,bed}$	64.04	Kg
$\dot{m}c_{p_{hw}}$	5.36	kW.K^{-1}
$\dot{m}c_{p_{cw}}$	6.36	kW.K^{-1}
$Mc_{p_{cond}}$	$24.38 \times 0.386 + 20 \times 4.186$	kJ.K^{-1}
$Mc_{p_{evap}}$	$12.45 \times 0.386 + 50 \times 4.186$	kJ.K^{-1}
UA_{bed}	4241.38	W.K^{-1}
UA_{cond}	15,349.80	W.K^{-1}
UA_{evap}	4884.90	W.K^{-1}
$\dot{m}_{cw}$	1.52	kg.s^{-1}
$\dot{m}_{hw,ch}$	1.28	kg.s^{-1}
$T_{cw,i}$	31	°C

3.4. System Performance Indicators

Performance of adsorption chillers in terms of cooling capacity and COP can be estimated using the following equations [17].

$$Q_C = \frac{\int_0^{t_{cyc}} \dot{m}_{ch} c_{Pch}(T_{ch,in} - T_{ch,out})dt}{t_{cyc}} \tag{20}$$

$$COP_{cyc} = \frac{\int_0^{t_{cyc}} \dot{m}_{ch} c_{Pch}(T_{ch,in} - T_{ch,out})dt}{\int_0^{t_{cyc}} \dot{m}_{hw} c_{Phw}(T_{hw,in} - T_{hw,out})dt} \tag{21}$$

The average overall system efficiency $\eta_{overall}$, predicated based on both the electricity generated and the cooling capacity, is estimated using Equation (2) below [33,34]. Also, it is worth noting that the electricity consumed by all pumps is negligible and, as such, has been neglected.

$$\eta_{overall} = \frac{\int_0^{t_{cyc}} \left[\dot{m}_{ch} c_{Pch}(T_{ch,in} - T_{ch,out}) + P_{el}\right]dt}{\int_0^{t_{cyc}} (A_{PVT} + A_{ETC}) I_t dt} \tag{22}$$

3.5. Model Validation

The mathematical model underwent validation using a wide range of influential components. As a sample and for demonstration purposes, computational results were juxtaposed with the experimental findings presented in Ref. [32] to validate the mathematical model for adsorption chillers. Notably, the model and experimental results exhibited a considerable degree of consistency. The comparison between the prediction values obtained by the mathematical model and the experimental data is illustrated in Figure 2.
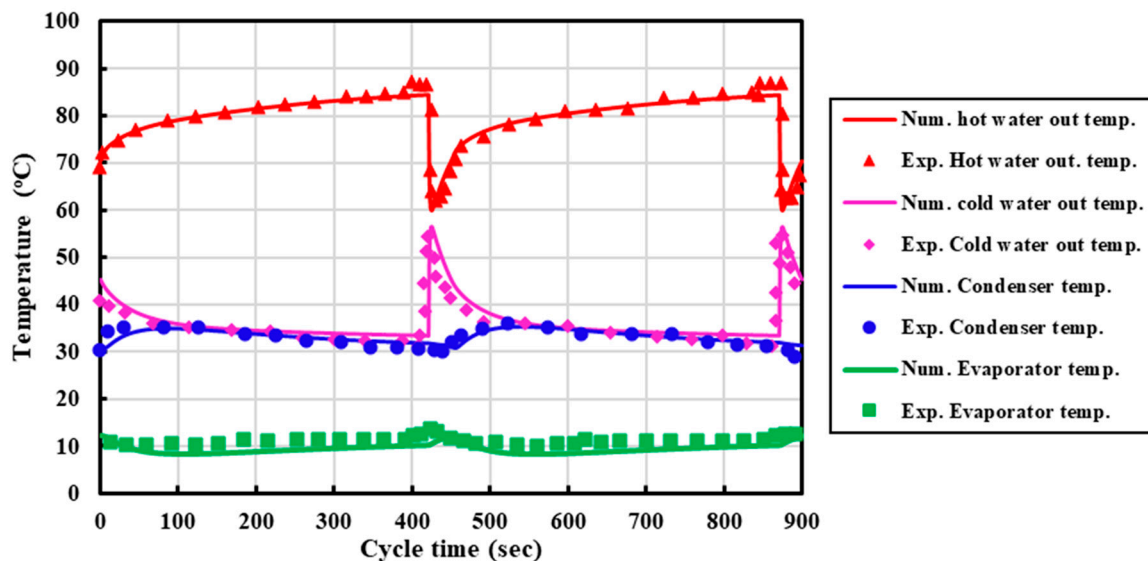
Figure 2. Mathematical model verification: the lines represent the present study and the dots represent experimental data from Ref. [32].

4. Results and Discussion

4.1. Climatic Data

Riyadh, Saudi Arabia (24.46° N, 46.44° E), Kuwait City, Kuwait (29.22° N, 47.59° E), and Sharjah, United Arab Emirates (25.2° N, 55.24° E) are the three cities investigated in the current study during June, July, and August. The three cities' climatic information, including the average temperature and solar radiation, was gathered from the National Solar Radiation Database (NSRDB). Figure 3 illustrates the daily I_t and T_{amb} on the day of 15 June 2019.
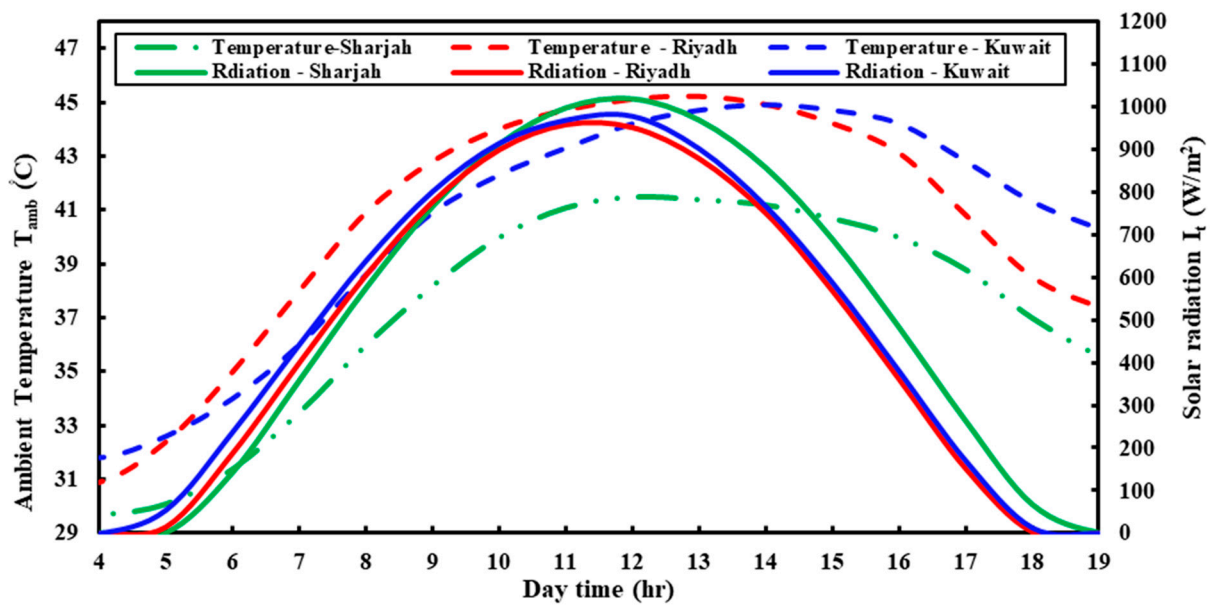
Figure 3. Climate conditions on the 15 June 2019.

4.2. System Performance

4.2.1. Adsorption Cooling System

In Figure 4, the temperature profiles of the system's condenser, evaporator, two adsorption beds, hot water storage tank, and other components are shown. The temperature profiles depicted in Figure 3 were selected between the hours of 14:00 and 15:00, which correspond to the maximal cooling capacity during the day.
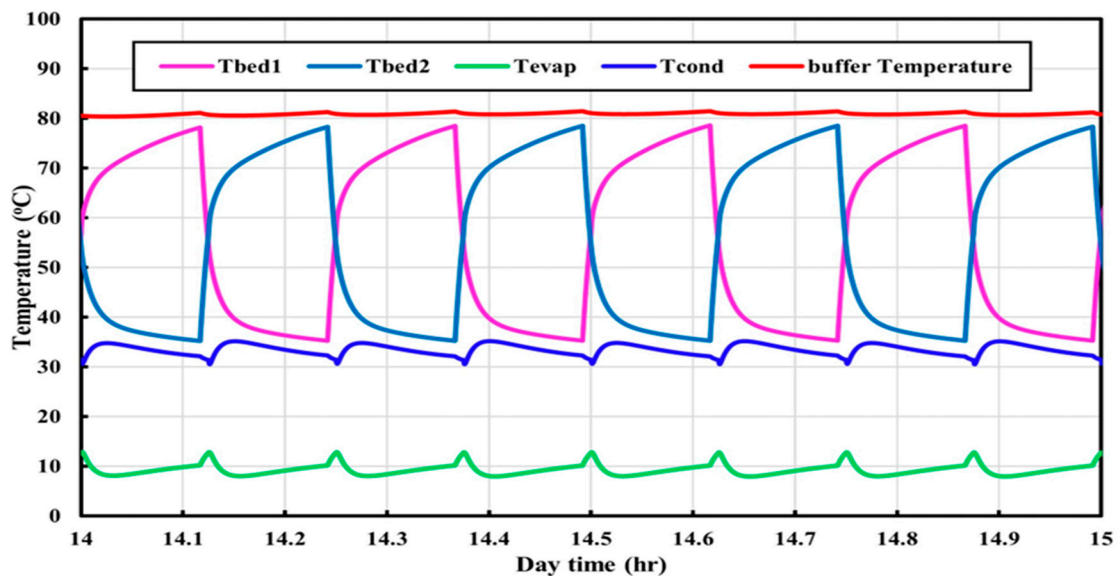
Figure 4. Temperature profiles throughout four cycles for the condenser, evaporator, two beds, and water tank.

As depicted in Figure 4, the average temperature of the hot water storage tank is approximately 80 °C, while the evaporator and condenser have average temperatures of about 10 °C and 32 °C, respectively. The average cooling capacity and COP of the adsorption cooling system throughout the three months of summer in the three different cities are reported in Figure 5.
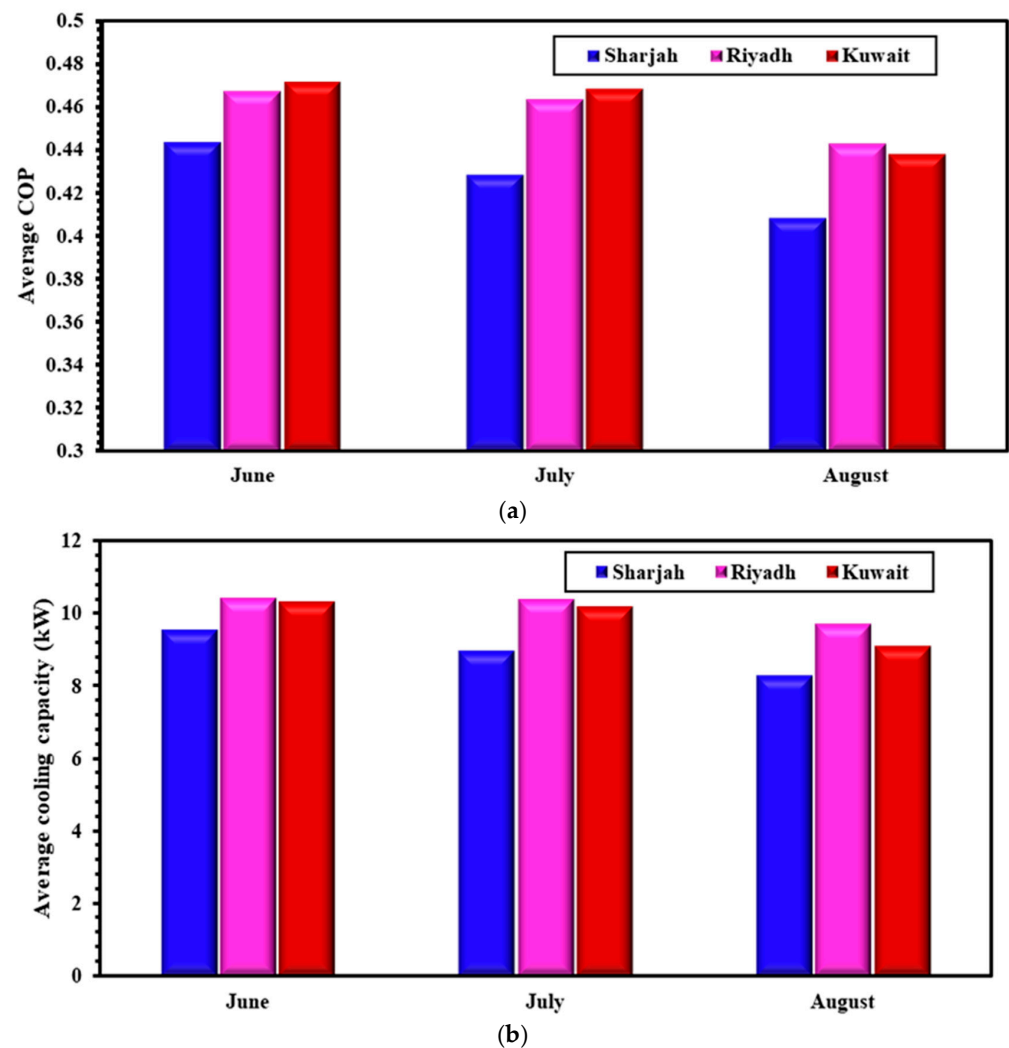
Figure 5. Average COP and cooling capacity of the adsorption chiller for the three months; (**a**) average COP, (**b**) average cooling capacity.

One can notice from Figure 5a,b that the best performance in terms of cooling capacity and COP is achieved in the month of June. Among the three cities tested, Kuwait City demonstrates a COP of 0.47 and a cooling capacity of 10.5 kW. Closely following this is Riyadh City, which shows a COP of 0.46 and a cooling capacity of 10.6 kW. Sharjah City demonstrates a COP value of 0.44 and a cooling capacity of 9.5 kW. This might be due to the fact that both Kuwait City and Riyadh have very similar climate conditions, specifically their high ambient temperature, as shown in Figure 3. Sharjah City was selected as a representative example to predict the performance of the adsorption cooling system throughout a typical day for each of the three tested months. The variation of the cooling capacity and COP over time is depicted in Figure 6a,b.

As expected, the cooling capacity increases with time until it reaches a maximum value at about 15:00. It then decreases with time until reaching a minimum value at the end of the day. One also can notice that the adsorption cooling system still can produce cooling after 19:00, due to the thermal inertia of the hot storage tank.

Figure 6b shows the variation of the COP with time for a typical day in each month. The COP of all months follows the same trend and reaches its maximum value between 16:00 and 18:00. The COP's trend over the three months mirrors the cooling capacity, as depicted in Figure 6b. The peak COP values for June, July, and August are 0.48, 0.47, and 0.45, respectively, showing minimal variation. Meanwhile, the average COP values for these months are 0.37, 0.35, and 0.34, as highlighted in Figure 6b.

(a)

(b)
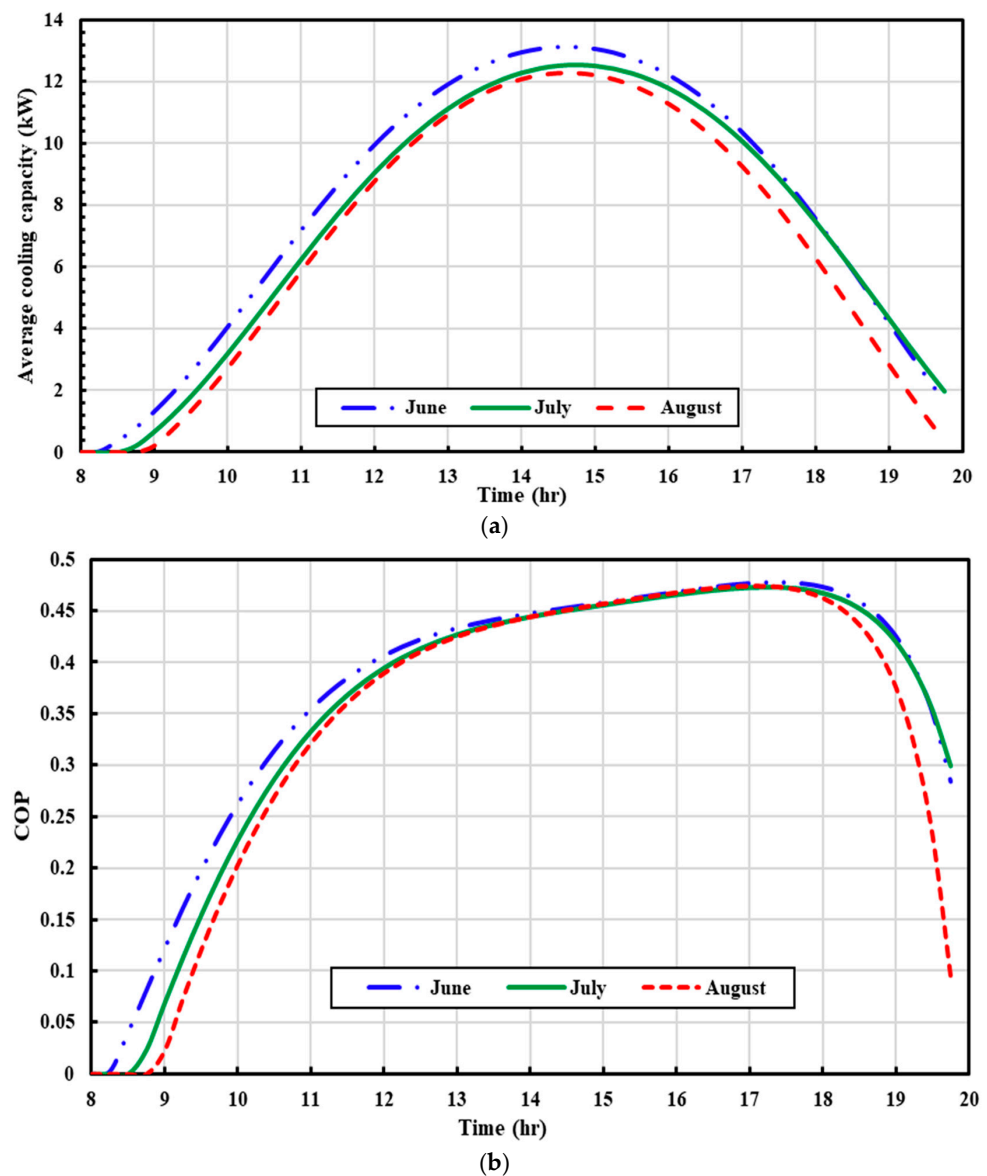
Figure 6. Variation of cooling capacity and COP over time for Sharjah city: (**a**) cooling capacity, (**b**) COP.

Figure 7 shows the plot of solar heating capacity and the adsorption chiller cooling capacity over time. It can be seen from Figure 7 that the solar heating capacity reaches its maximum between 12:00 and 13:00, whilst the maximum cooling capacity is achieved between 14:00 and 15:00. It is also worth mentioning that the heating capacity approaches zero at about 19:00 at sunset, while the cooling capacity persists after sunset due to the thermal inertia of the buffer tank.

4.2.2. The Generated Electrical Power

Figure 8 shows the electrical power generated by the PVT collectors in the three cities during a typical day in June. As shown in Figure 8, the electrical power in the three cities follows the same pattern, steadily rising from the early morning and reaching its peak at midday. It then gradually decreases until it reaches a minimum value at the end of the day. In general, it was found that the values of power generated in all cities are similar, with only slight differences. It can be seen from Figure 6 that the electrical power generated by the PVT collectors in Sharjah is lower than that in Riyadh and Kuwait City during the

morning. However, after approximately the 13:00, the power generated in the three cities becomes very similar, with a slightly higher value in Sharjah.
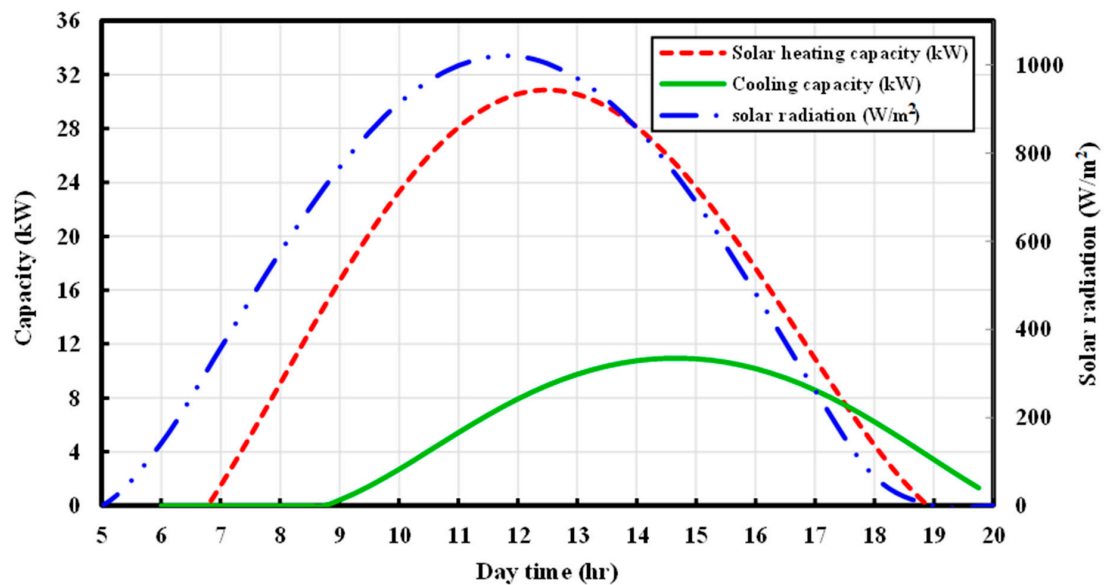
Figure 7. Variation of solar radiation, solar heating capacity and cooling capacity over time for Sharjah city on the 15 June 2019.
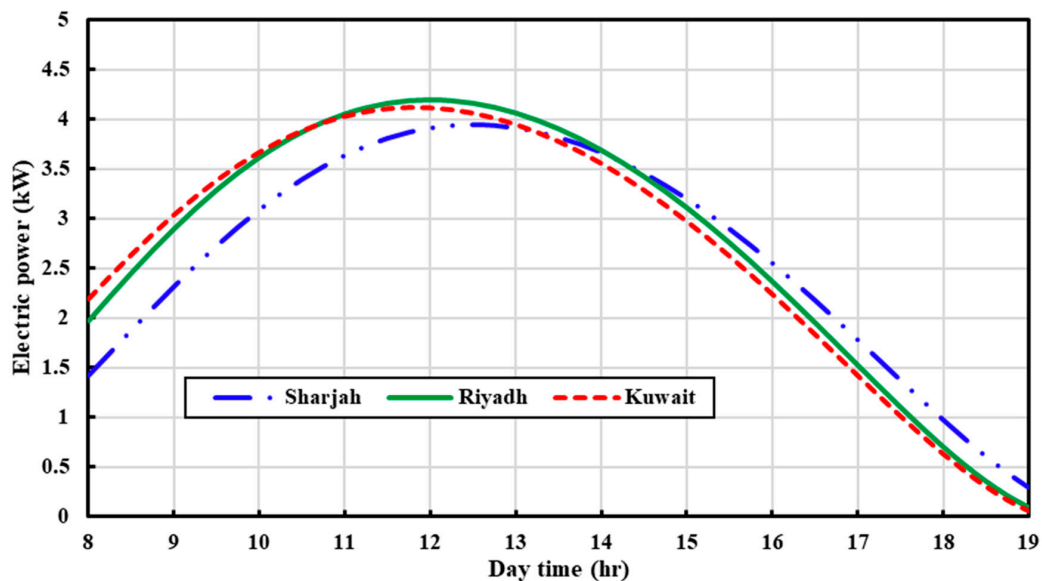
Figure 8. PVT-generated electricity on the 15 June 2019 in the three cities.

The average daily electrical energy generated throughout the three summer months in the studied cities is presented in Figure 9. As shown in Figure 9, Riyadh exhibits the highest electrical energy generation throughout all three months. Specifically, the month of June demonstrates the maximum electrical energy values generated from the PVT system in all three cities. In greater detail, in June, Riyadh achieves the highest average daily energy generation of 33.05 kWh, closely followed by Sharjah, with 32.81 kWh, and Kuwait City, with 32.69 kWh. Conversely, the month of August showcases the lowest electrical energy values for the three cities, with Riyadh averaging 31.69 kWh/day, followed by Kuwait City, with 30.21 kWh/day and Sharjah, with 30.00 kWh/day.

Figure 10 presents the total system efficiency for all cities under investigation during a typical day in June, in which both cooling and electrical power generation are considered.

As can be seen from Figure 10, for all cities under investigation, the system overall efficiency has the same trend. It increases generally with time until about 17:00. After that, one can notice that there is a sharp increase in the system's overall efficiency, thanks to the thermal energy stored in the hot water tank that drives the adsorption cooling system during the afternoon period, when the intensity of solar radiation decreases.
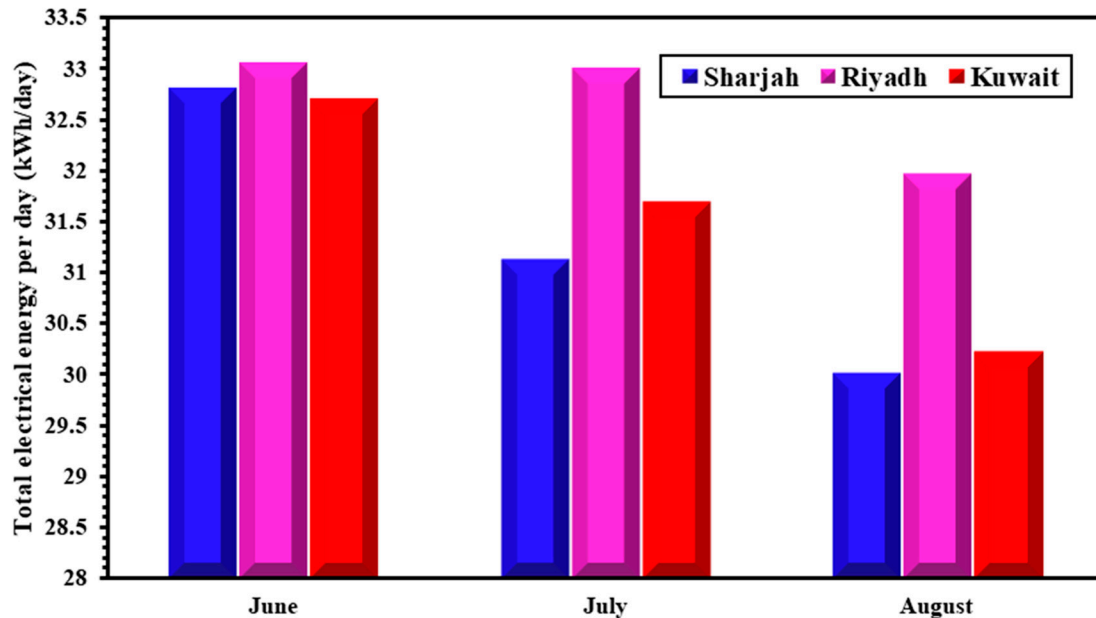
Figure 9. Total electrical generated energy per day for the three months.
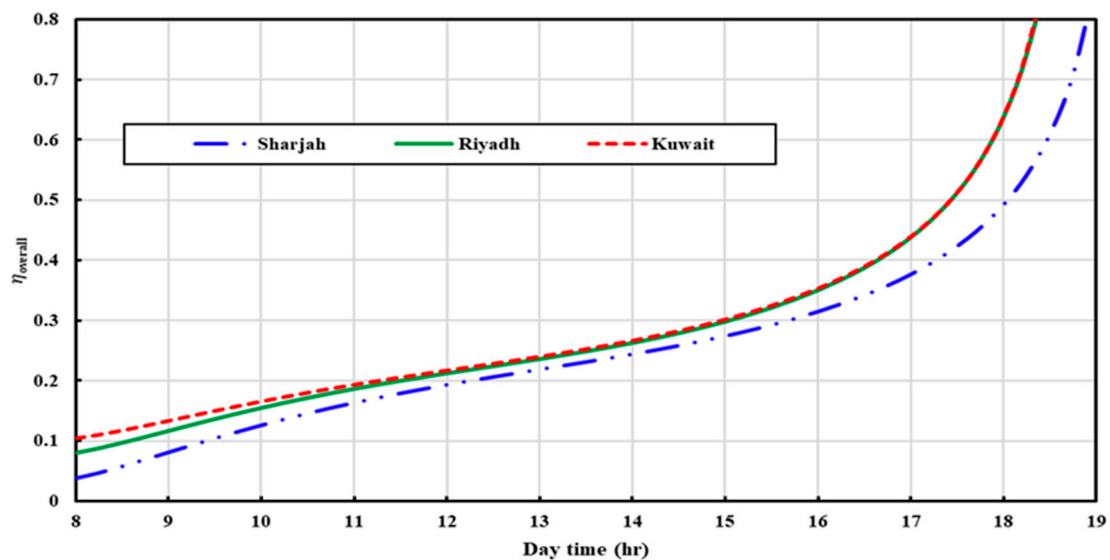
Figure 10. Total system efficiency for all cities under investigation on the 15 June 2019.

5. Comparison with Other Related Studies

Table 4 depicts a comparison between the current study and some other related studies available in the literature.

It should be highlighted that the system's performance was assessed within the specific climatic conditions of GCC countries. Therefore, generalizing these findings to different regions may be affected by variations in climate and environmental factors. Furthermore, it is worth noting that factors related to the long-term durability of the system and its economic analysis are beyond the scope of the present study and need further research.

Table 4. Comparison between the current study and the antecedent studies of relevance.

Reference	Description	Main Findings
Calise et al. [19]	• Dynamic simulation of a polygeneration system has been introduced. • The system includes PVT collectors, a heat pump, an adsorption chiller, and energy storage.	• Share of electrical energy storage system: 20%. • Simple pay-back period: 15 years (best configuration).
El-Sharkawy et al. [20]	• The performance of the two-bed adsorption cooling system has been investigated theoretically using the climate conditions of the Middle East. • Concentrated parabolic trough collectors have been used to drive the adsorption chillers. • Three cities were chosen for this study, namely Cairo and Aswan located in Egypt and Jeddah in Saudi Arabia.	• Maximum cyclic average cooling capacity reaches about 14.8 kW for a system working under the climate conditions of Cairo and Jeddah. It reached about 15.8 kW for Aswan City.
Aneli et al. [35]	• The effectiveness and constraints of using PVT collectors to drive an adsorption chiller were theoretically investigated. • Comparison between the adsorption chiller driven by PVT collectors with a vapor compressor system driven by PV collectors is discussed.	• Results show the superiority of the vapor compressor system driven by PV collectors, as it produces about 2.9 kWh more cooling energy than the PVT-powered adsorption chiller.
Zhai and Wang [36]	• This study examines the performance of an adsorption cooling system, driven by evacuated tube collectors. • Two configurations, namely with and without a heat storge tank, are presented and their performance is evaluated.	• The use of heat storage makes the operation more stable • The configuration without heat storage has higher efficiency and COP
Hassan et al. [17]	• Utilizing the climate conditions of Alexandria, Egypt, the authors conducted a study to analyze the theoretical performance of a solar-driven adsorption-based trigeneration system. • The system's performance was assessed across five configurations of the PVT/ETC collectors.	• Using only ETCs with a parallel connection results in the highest average cooling capacity and COP. • Among the tested months, the best system performance was obtained in August for all of the proposed configuration of the PVT/ETC collectors.
Current study	• An adsorption-based system for the simultaneous production of cooling and electricity is n presented. • The system performance is theoretically investigated under the climate conditions of the GCC. • The system is driven using a combination of the PVT/ETC. This combination has been selected based on one of our previous studies.	• Among the three cities tested in this study, Riyadh in Saudi Arabia shows better performance. • Considering the electrical energy produced by the PVT collectors in the three cities, it is found that Riyadh produced the highest amount, followed by Kuwait City and then Sharjah.

6. Conclusions

In this study, we theoretically examined the performance of a novel solar-driven, adsorption-based multi-generation system tailored for the climatic conditions of GCC countries. The proposed configuration leverages the optimal blend of PVT and ETC

collectors both to power an adsorption chiller and to generate electricity. Three cities have been selected for this study, namely Kuwait City in Kuwait, Sharjah in UAE and Riyadh in Saudi Arabia. This study was conducted during the three months in the summer season, namely June, July, and August, considering the weather conditions of the three cities under investigation. The main findings can be summarized as follows:

- The Gulf region experiences hot climate conditions during summer, with a solar radiation level approaching 1000 W/m^2, making it an attractive location for implementing solar cooling systems.
- Among the three cities tested in this study, Riyadh in Saudi Arabia shows better performance due to its relatively higher solar radiation levels and ambient temperatures. On a typical day in June, the adsorption cooling system in the three cities produced an average cooling capacity of 10.6, 10.5, and 9.5 kW in Riyadh, Kuwait, and Sharjah, respectively, while the average COP was found to be 0.464, 0.47, and 0.44, respectively.
- Considering the electrical energy produced by the PVT collectors in the three cities, it is found that Riyadh produced the highest amount, followed by Kuwait and then Sharjah. The total electrical energy generated by these cities was 31.65, 31.3, and 30.24 kWh/day, respectively.
- Considering the electrical energy produced by the PVT collectors in the three cities, it was found that Riyadh exhibits the highest level of electrical energy generation throughout all three months. Riyadh produced 33.05 kWh/day in June, 32.99 kWh/day in July, and 31.91 kWh/day in August.
- The month of June demonstrates the maximum electrical energy values generated from the PVT system in all three cities. Conversely, August showcases the lowest electrical energy values across the three cities, with Riyadh averaging 31.99 kWh/day, followed by Kuwait with 30.21 kWh/day, and Sharjah with 30.00 kWh/day.
- Irrespective of the city, including a storage tank and its connection to the adsorption chiller enhances the system's overall efficiency, particularly during the late daylight hours, with the system efficiency reaching approximately 0.64.

Author Contributions: Conceptualization, I.I.E.-S.; methodology, I.I.E.-S. and M.H.; software, M.H.; validation, I.I.E.-S., M.H. and M.M.A.-E.; data curation, I.I.E.-S., M.H. and M.M.A.-E.; writing—review and editing, I.I.E.-S., M.M.A.-E., A.R. and A.I.; project administration, I.I.E.-S. All authors have read and agreed to the published version of the manuscript.

Institutional Review Board Statement: Not applicable.

Informed Consent Statement: Not applicable.

Data Availability Statement: Data available upon request from the authors.

Conflicts of Interest: The authors declare no conflict of interest.

Abbreviations

COP	coefficient of performance
ETC	evacuated tube solar collectors
GCC	Gulf Cooperation Council
IIR	International Institute of Refrigeration
LDF	linear driving force
LMTD	logarithmic mean temperature difference
PV	photovoltaic
PVT	photovoltaic-thermal solar collectors
RD	regular density
STC	standard testing condition
UAE	United Arab Emirates

Nomenclature

A	*area (m^2)*
A_n	constants in Equation (13)
B_n	constants in Equation (14)
C_P	specific heat capacity (kJ kg^{-1} K^{-1})
D_{so}	pre-exponential constant (m^2 s^{-1})
E_a	activation energy (J mol^{-1})
I_t	incident solar radiation (W m^{-2})
K	mass transfer coefficient (m^2 s^{-1})
m	mass (kg)
$\dot{m}$	mass flow rate (kg s^{-1})
P_{el}	electrical power
P	pressure (kPa)
Q_c	mean cooling capacity of cycle (kW)
Q_{st}	isosteric heat of adsorption (kJ kg^{-1})
R	universal gas constant (kJ kmol^{-1} K^{-1})
r_p	adsorbent particle radius (m)
T	temperature (K)
t	Time (s)
W_{eq}	amount adsorbed at equilibrium condition (kg kg^{-1})
w	instantaneous adsorption uptake (kg kg^{-1})
U	heat transfer coefficient (W m^{-2}K^{-1})

Greek letters

α	absorber solar absorptivity
β	power's temperature coefficient
γ	intercept factor
η	Efficiency
ρ	mirror reflectivity
τ	cover transmittance

Subscripts

Ad	adsorption/adsorbent
Amb	ambient
Bed	adsorber/desorber bed
Ch	chilled water
C	condenser cooling water
Con	condenser
Cw	cooling water
Cyc	cycle
De	desorption
El	electrical
Eva	evaporator
Hw	hot water
HE	heat exchanger
In	inlet
$mean$	mean value
Out	outlet
Ref	reference
Sat	saturation
$s.c$	solar collector system
$s.t$	storage tank
T	tilted surface
Th	thermal

References

1. Murugan, S.; Horák, B. Tri and Polygeneration Systems—A Review. *Renew. Sustain. Energy Rev.* **2016**, *60*, 1032–1051. [CrossRef]
2. Papakokkinos, G.; Castro, J.; Capdevila, R.; Damle, R. A Comprehensive Simulation Tool for Adsorption-Based Solar-Cooled Buildings—Control Strategy Based on Variable Cycle Duration. *Energy Build* **2021**, *231*, 110591. [CrossRef]

3. Key World Energy Statistics 2021. In *Report of the International Energy Agency 2021*; International Energy Agency: Paris, France, 2021. Available online: https://www.iea.org/reports/key-world-energy-statistics-2021 (accessed on 8 July 2023).

4. Dupont, J.L.; Domanski, P.; Lebrun, P.; Ziegler, F. The Role of Refrigeration in the Global Economy. In Proceedings of the 38th Note on Refrigeration Technologies (International Institute of Refrigeration, 2019), Montreal, QC, Canada,, 24–30 August 2019.

5. Cooling. *Report of the International Energy Agency*; International Energy Agency: Paris, France, 2021. Available online: https://www.iea.org/reports/cooling (accessed on 8 July 2023).

6. Mas' ud, A.A.; Wirba, A.V.; Alshammari, S.J.; Muhammad-Sukki, F.; Abdullahi, M.A.M.; Albarracín, R.; Hoq, M.Z. Solar energy potentials and benefits in the gulf cooperation council countries: A review of substantial issues. *Energies* **2018**, *11*, 372. [CrossRef]

7. Zarei, A.; Liravi, M.; Rabiee, M.B.; Ghodrat, M. A Novel, Eco-Friendly Combined Solar Cooling and Heating System, Powered by Hybrid Photovoltaic Thermal (PVT) Collector for Domestic Application. *Energy Convers Manag.* **2020**, *222*, 113198. [CrossRef]

8. Akhtar, S.; Khan, T.S.; Ilyas, S.; Alshehhi, M.S. Feasibility and Basic Design of Solar Integrated Absorption Refrigeration for an Industry. *Energy Procedia* **2015**, *75*, 508–513. [CrossRef]

9. Wang, D.C.; Wang, Y.J.; Zhang, J.P.; Tian, X.L.; Wu, J.Y. Experimental Study of Adsorption Chiller Driven by Variable Heat Source. *Energy Convers. Manag.* **2008**, *49*, 1063–1073. [CrossRef]

10. Bagherian, M.A.; Mehranzamir, K. A Comprehensive Review on Renewable Energy Integration for Combined Heat and Power Production. *Energy Convers. Manag.* **2020**, *224*, 113454. [CrossRef]

11. Kasaeian, A.; Bellos, E.; Shamaeizadeh, A.; Tzivanidis, C. Solar-Driven Polygeneration Systems: Recent Progress and Outlook. *Appl. Energy* **2020**, *264*, 114764. [CrossRef]

12. Wang, J.; Han, Z.; Guan, Z. Hybrid Solar-Assisted Combined Cooling, Heating, and Power Systems: A Review. *Renew. Sustain. Energy Rev.* **2020**, *133*, 110256. [CrossRef]

13. Herez, A.; El Hage, H.; Lemenand, T.; Ramadan, M.; Khaled, M. Review on Photovoltaic/Thermal Hybrid Solar Collectors: Classifications, Applications and New Systems. *Sol. Energy* **2020**, *207*, 1321–1347. [CrossRef]

14. Joshi, S.S.; Dhoble, A.S. Photovoltaic -Thermal Systems (PVT): Technology Review and Future Trends. *Renew. Sustain. Energy Rev.* **2018**, *92*, 848–882. [CrossRef]

15. Liu, M.; Shi, Y.; Fang, F. Combined Cooling, Heating and Power Systems: A Survey. *Renew. Sustain. Energy Rev.* **2014**, *35*, 1–22. [CrossRef]

16. Mohammadi, K.; Khanmohammadi, S.; Khorasanizadeh, H.; Powell, K. A comprehensive review of solar only and hybrid solar driven multigeneration systems: Classifications, benefits, design and prospective. *Appl. Energy* **2020**, *268*, 114940. [CrossRef]

17. Hassan, A.A.; Elwardany, A.E.; Ookawara, S.; El-Sharkawy, I.I. Performance Investigation of a Solar-Powered Adsorption-Based Trigeneration System for Cooling, Electricity, and Domestic Hot Water Production. *Appl. Therm. Eng.* **2021**, *199*, 117553. [CrossRef]

18. Motamedi, S.; Mehdipour Ghazi, M.; Moradi, S.; Talaie, M.R. An Economic Investigation of a Solar-Powered Adsorption Cooling System. *ChemEngineering* **2022**, *6*, 81. [CrossRef]

19. Calise, F.; Figaj, R.D.; Vanoli, L. A Novel Polygeneration System Integrating Photovoltaic/Thermal Collectors, Solar Assisted Heat Pump, Adsorption Chiller and Electrical Energy Storage: Dynamic and Energy-Economic Analysis. *Energy Convers. Manag.* **2017**, *149*, 798–814. [CrossRef]

20. El-Sharkawy, I.I.; AbdelMeguid, H.; Saha, B.B. Potential Application of Solar Powered Adsorption Cooling Systems in the Middle East. *Appl. Energy* **2014**, *126*, 235–245. [CrossRef]

21. Papoutsis, E.G.; Koronaki, I.P.; Papaefthimiou, V.D. Numerical Simulation and Parametric Study of Different Types of Solar Cooling Systems under Mediterranean Climatic Conditions. *Energy Build* **2017**, *138*, 601–611. [CrossRef]

22. Mostafa, A.; Hassanain, M.; Elgendy, E. Transient Simulation and Design Parameters Optimization of a Cold Store Utilizes Solar Assisted Adsorption Refrigeration System. *Case Stud. Therm. Eng.* **2022**, *37*, 102273. [CrossRef]

23. Apricus ETC-20 Evacuted Tube Collector. Available online: https://www.apricus.com/ETC-20-Solar-Collector-pd46805927.html (accessed on 11 July 2023).

24. FOTOTHERM PVT AL-Series Collectors. Available online: https://www.fototherm.com/en/ourproducts/. (accessed on 11 July 2023).

25. Lämmle, M.; Kroyer, T.; Fortuin, S.; Wiese, M.; Hermann, M. Development and Modelling of Highly-Efficient PVT Collectors with Low-Emissivity Coatings. *Sol. Energy* **2016**, *130*, 161–173. [CrossRef]

26. Buonomano, A.; Calise, F.; Palombo, A.; Vicidomini, M. Adsorption Chiller Operation by Recovering Low-Temperature Heat from Building Integrated Photovoltaic Thermal Collectors: Modelling and Simulation. *Energy Convers. Manag.* **2017**, *149*, 1019–1036. [CrossRef]

27. López-Martín, R.; Valenzuela, L. Optical Efficiency Measurement of Solar Receiver Tubes: A Testbed and Case Studies. *Case Stud. Therm. Eng.* **2018**, *12*, 414–422. [CrossRef]

28. Evola, G.; Marletta, L. Exergy and Thermoeconomic Optimization of a Water-Cooled Glazed Hybrid Photovoltaic/Thermal (PVT) Collector. *Sol. Energy* **2014**, *107*, 12–25. [CrossRef]

29. Askalany, A.A.; Saha, B.B.; Ahmed, M.S.; Ismail, I.M. Adsorption Cooling System Employing Granular Activated Carbon–R134a Pair for Renewable Energy Applications. *Int. J. Refrig.* **2013**, *36*, 1037–1044. [CrossRef]

30. Saha, B.B.; Koyama, S.; Kashiwagi, T.; Akisawa, A.; Ng, K.C.; Chua, H.T. Waste heat driven dual-mode, multi-stage, multi-bed regenerative adsorption system. *Int. J. Refrig.* **2003**, *26*, 749–757. [CrossRef]

31. Elsheniti, M.B.; Rezk, A.; Shaaban, M.; Roshdy, M.; Nagib, Y.M.; Elsamni, O.A.; Saha, B.B. Performance of a Solar Adsorption Cooling and Desalination System Using Aluminum Fumarate and Silica Gel. *Appl. Therm. Eng.* **2021**, *194*, 117116. [CrossRef]
32. Saha, B.B.; Boelman, E.C.; Kashiwagi, T. Computer Simulation of a Silica Gel-Water Adsorption Refrigeration Cycle-the Influence of Operating Conditions on Cooling Output and COP. *ASHRAE Trans.* **1995**, *101*, 348–357.
33. Zhai, H.; Dai, Y.J.; Wu, J.Y.; Wang, R.Z. Energy and Exergy Analyses on a Novel Hybrid Solar Heating, Cooling and Power Generation System for Remote Areas. *Appl. Energy* **2009**, *86*, 1395–1404. [CrossRef]
34. Koronaki, I.P.; Papoutsis, E.G.; Papaefthimiou, V.D. Thermodynamic Modeling and Exergy Analysis of a Solar Adsorption Cooling System with Cooling Tower in Mediterranean Conditions. *Appl. Therm. Eng.* **2016**, *99*, 1027–1038. [CrossRef]
35. Aneli, S.; Gagliano, A.; Tina, G.M.; Ilis, G.G.; Demir, H. Effectiveness and Constraints of Using PV/Thermal Collectors for Heat-Driven Chillers. *Appl. Therm. Eng.* **2022**, *210*, 118330. [CrossRef]
36. Zhai, X.Q.; Wang, R.Z. Experimental Investigation and Performance Analysis on a Solar Adsorption Cooling System with/without Heat Storage. *Appl. Energy* **2010**, *87*, 824–835. [CrossRef]